Optimal sizing and siting of smart microgrid components under high renewables penetration considering demand response

Optimal Sizing and Siting of Smart Microgrid Components under High Renewables Penetration Considering Demand Response

Seyed Mehdi Hakimi[a], Arezoo Hasankhani[b], Miadreza Shafie-khah[c,*], João P.S. Catalão[d]

[a] *Electrical Engineering Department, Damavand Branch, Islamic Azad University, Damavand, Iran*
[b] *Electrical Engineering Department, Amirkabir University of Technology, Tehran, Iran*
[c] *School of Technology and Innovations, University of Vaasa, 65200 Vaasa, Finland*
[d] *Faculty of Engineering of the University of Porto and INESC TEC, 4200-465 Porto, Portugal*

Abstract: The purpose of this article is to determine the size and place of different components in microgrids (MGs) including renewable energy resources (RERs). Various factors like reliability, uncertainty of wind speed, solar irradiance, load and load growth are considered. The Ekbatan residential complex is studied as the pilot case study placed in Tehran, Iran. Ekbatan complex has three separate sets of buildings called phase 1, 2 and 3 considered as smart MGs. The multi-objective optimization problem is solved considering RERs uncertainties, improving reliability and power quality and minimizing power loss by particle swarm optimization (PSO) algorithm. Different constraints in terms of voltage and frequency as well as resources and ESSs capacity are taken into consideration. The effect of load growth, photovoltaic (PV) and energy storage systems (ESSs) placement, changing the capital cost of RERs and demand response (DR) of controllable loads are studied on optimal sizing and siting. The proposed method is tested on a WT/PV/FC/hydrogen tank MGs system, and the optimal sizing and siting of mentioned sources can decelerate the rate of increase in the total cost of MG considering the load growth.

Nomenclature

NPC	Net present cost
N	Number (unit) or the capacity of components
CC	Capital cost (US$/unit)
RC	Replacement cost (US$/unit)
$O\&MC$	Annual operation and maintenance cost (US$/unit-year)
R	Project lifetime
Ir	Real interest rate
$ir_{nominal}$	Nominal interest rate
$Fuel_{cost}$	Cost of fuel which is only considered for MT
F	Annual inflation rate
PWA	Annual payment present worth
K	Single payment present worth
L	Useful life of a specified components
Y	Replacement number of specified components
C_{shedd}	Average of penalty cost to load curtailment (US$/kWh)
I	Components in smart MG
$NPC_{SA,\ n}$	Net present value of the surplus investment cost of the nth smart components
$\sum NPC_{Trans}$	Net present cost value of distribution transformer
$NPC_{incentive.n}$	Net present value of nth smart appliances incentive
$SACi$	Surplus cost which should be paid for ith appliance (e.g., washing machine).
$N\ (start-ave)_i$	Average usage number of ith smart appliance for one year
$N\ (avl)$	Number that ith appliance is available
$N\ (shift)_i$	Shifting number of ith appliance annually
$P_{buy}(t)\ /\ P_{sell}(t)$	Amount of power bought/sold from/to the network at t
$Price_{buy}(t)$	Price of electricity bought from distribution network per kWh
$Price_{sell}(t)$	Price of electricity sold to distribution network per kWh
θ_{PV}	Installation angle of the PV array
$N_{TR}(max)$	Maximum capacity of distribution transformer
ELF	Equivalent loss Factor
$Q(t)$	Amount of load which is lost (is not supplied) (kWh)
$D(t)$	Amount of demand (kWh)
$REPP$	Renewable energy penetration percentage
$P_{REN\text{-}Direct}$	Produced power of the RERs
$V_j(t)$	Voltage of bus jth at t
$P_{loss}\ /\ Q_{loss}$	Active/reactive power loss
$P_{Dj}(t)\ /\ P_{DGj}(t)$	Active power consumed and produced respectively in jth bus at t
$Q_{DGj}(t)\ /\ Q_{Dj}(t)$	Reactive power consumed and produced respectively in jth bus at t
TC_{ij}	Total cost of movement including lost energy and cost of changing location
DC_{iab}	Cost of changing location ith DG from location (a) at (j-1)th year to location (b) at (j)th year
LDG_{ij}	Cost of lost energy
$h_{i.trans}$	Required time for transporting ith DG
EP_j	Price of buying energy at jth year from distribution grid
$G_{i.rated}$	Rated power of ith DG
N_{bus}	Possible places for installation of DG
N_{DG}	Number of DG types
a	Load growth rate
LP_0	Initial peak load
LP_j	Peak load at jth year

1. Introduction

In a smart microgrid (MG), when wind turbine (WT), photovoltaic cell (PV), backup system, energy storage system (ESS) and demand response (DR) resources are used, the optimization problem is too complex. It is because of calculating the power of the mentioned sources with the objective function that minimizes the total cost and power loss, while improves reliability and power quality.

The power of the backup system should be considered in an acceptable amount to supply the emergency loads because of the intermittent nature of RERs. MGs connected to a network are able to sell/buy energy from/to the network, which increases the complexity of the optimization problem that should be solved at all hours of the day. RERs development has a destructive effect on financial, reliability and DR aspects. These problems can mitigate by optimal sizing and siting of RERs, which is also suitable in minimizing the loss and increasing the competitiveness of RERs. Different resources have studied the importance of the optimal placement and sizing of RERs.

In [1], the optimal sizing of RERs has been carried out for an industrial MG considering the techno-economic optimization. A genetic algorithm has been applied in [1], and the optimal size of RERs was determined considering cogeneration for compensation of intermittent behavior of RERs. In [2], the optimal size of ESSs has been determined for WTs considering the statistical modeling based on vine-copula theory although economic aspects were not considered. In [3], the optimal place and size of DGs have been investigated to minimize the total cost of an active distribution network, and the problem was solved by CVX platform and GUROBI solver. The optimal placement and sizing of DGs have been carried out by chaos embedded SOS algorithm in a radial distribution network with the objective of decreasing the power loss and improving the voltage stability [4].

Different methods have been developed for RERs optimal sizing and siting in distribution grids. References [5] and [6] address a method for optimal location and capacity of DGs considering their intermittent nature. In [7], the substation has been optimally sized and sited with minimum investment, annual operation costs and the cost of land for developed urban areas. In [8], two important factors including maximum reliability and minimum cost have been considered, and the optimal size and place of WT, PV and battery ESS have been determined. Two constraint-based iterative search algorithms have been introduced in [8] , in which the first algorithm was applied for sources sizing while the second algorithm was used for the battery sizing. The optimal place and capacity of WT, PV and batteries have been similarly specified based on minimizing the total cost [9], in addition to cost and environmental considerations [10].

Determining the ESS size and place is an important problem in smart MGs. In [11], the optimal size of PV and ESS has been investigated to meet the anaerobic digestion generator and PV constraints with the objective to minimize the levelized cost of energy. In [12], the optimal sizing of PV/diesel with the aim of minimizing cost and improving reliability has been studied, and the optimization problem was solved by a levy flight-based PSO. The optimal location and capacity of ESS have been determined in [13], [14] and [15] to achieve the goals of cost minimization, reliability improvement and load shaving. In [16], a multi-criteria method has been proposed to optimally size WT, PV, FC, electrolyzer, Hydrogen tank and batteries, although the annual cost and the sources movement have not been considered. In [17], the optimal size of PV and hydro turbine has been determined based on dynamic programming with the objective to minimize the total cost and power system loss.

Different objectives like cost minimization have been considered in the literature for the optimization problem. The optimal size of PV, WT and ESS has specified in [18], [19] and [20] to minimize the total cost. In [21], the optimization model based on second-order conic programming problem has been presented for sizing and siting RERs, electric vehicle charging stations and ESSs. In [22], the novel method for sizing batteries with the objective of decreasing the load uncertainty considering the intermittent nature of wind has been addressed. In [23], a 3-level learning automata-based methodology in a master-slave structure has been studied for RERs siting and sizing. The annual forecasted cost has not been considered in these references.

Considering DR programs are important in determining the site and size of RERs and ESSs. The optimal place and size of plug-in electric vehicles charging stations have been specified by using genetic algorithm method with embedded Monte Carlo simulation in [24]. The incentive-based DR has been considered in optimal placement and size of electric vehicle charging stations, which has been handled by PSO [25].

DR programs have been implemented by different objectives. In [26], the effect of DR on RERs sizing including WT and PV has been studied to minimize the peak hourly energy consumption. The impact of DR programs on PV-based system management has been addressed in [27]. DR programs and energy storages have been applied to replace conventional fuels with RERs [28]. Although the effect of DR on the optimal sizing and siting of electric vehicle charging stations and limited effects on the optimal sizing of WT/PV have been studied, the impact of DR of controllable loads on optimal placement and sizing of RERs and ESSs have not been addressed.

The contribution of the study can be listed as follows:

- MGs' loads are increasing each year, so new components should be added to MGs for supplying this load growth. The added components at ith year will produce power during (n-i+1) years in which *n* shows the lifetime of the project. The optimal capacity and location of each source should be annually computed. In this paper, the different load growth in developing buses comparing to non-developing ones is considered.
- The capital cost of RERs is decreasing over the time, so one of the novelties in this study is considering the different annual forecasted capital cost in optimization problem at each year, which makes the calculations more realistic.
- Considering the effect of DR of controllable loads and power quality in optimal sizing and siting of RERs

The rest of the paper is organized as follows. Section 2 provides the details of the Modeling optimal sizing and siting components in MGs. Section 3 is devoted to

simulation and result discussion. Finally, section 4 provides some relevant conclusions.

2. Modeling optimal sizing and siting components in MGs

In this section, the optimal size and place of RERs and ESSs are specified simultaneously. The objective function in this study minimizes the cost of sizing and siting of WT/PV/ESSs/FC/Hydrogen tank, which are explained as follows.

The assumptions of this study are as follows:

- Each phase in the Ekbatan complex is considered as an MG, and it is assumed that smart homes are equipped with smart meters and internet in order to transfer the information.
- All consumers in MGs use smart washing machine, smart dishwasher, smart heating/cooling system and plug-in electric vehicles.
- The smart equipment is placed at the start of the project, but power resources can be sited based on requirements.
- WTs and PV systems can be disconnected.
- WTs cannot be moved during the project.
- In the load flow calculations, WT and PV are considered with the fixed power factor.
- The installation and preparation cost of a new place for DGs is assumed 20% of their initial cost.
- In this study, the load growth is saturated after 10 years.

2.1. The optimal sizing

The purpose of this section is to optimize the size of components in MGs, i.e., the number of WTs, PVs, the capacity of electrolyzer, hydrogen tank, fuel cell (FC), micro turbine, batteries and DC/AC converter should be specified. The cost of the system includes investment net present cost (NPC), operation and maintenance, fuel, component replacement, smart devices, incentives related to participation in DR programs, buying and selling electricity and any cost related to power interruption over 20-year life cycle. In this problem, the constraint is the maximum allowable quantity for the reliability index ELF. However, some constraints related to maximum and minimum power and energy are considered.

The *NPC* related to component i can be calculated as follows:

$$NPC_i = N_i \times \left(CC_i + RC_i \times K_i + (Fuel_{costi} + \mathrm{O\&}MC_i) \times \mathrm{PWA(ir.R)}\right) \quad (1)$$

where, *N* is the number (unit) or the capacity of components (kW or kg), *CC* is the capital cost (US$/unit), *RC* shows the replacement cost (US$/unit), *O & MC* determines the annual operation and maintenance cost (US$/unit-year), *R* is the project lifetime, which is assumed 20 years in this study, *ir* is the real interest rate (i.e., 6% in this paper) which can be calculated based on the nominal interest rate ($ir_{nominal}$) and annual inflation rate (*f*). $Fuel_{costi}$ shows the cost of fuel which is only considered for MT, and it is assumed 0 for other DGs.

$$\mathrm{ir} = \frac{(ir_{nominal} - f)}{(1+f)} \quad (2)$$

PWA and *K* indicate the annual payment present worth and the single payment present worth, respectively:

$$\mathrm{PWA(ir.R)} = \frac{(1+ir)^R - 1}{ir(1+ir)^R} \quad (3)$$

$$K_i = \sum_{n=1}^{y_i} \frac{1}{(1+ir)^{n \times L_i}} \quad (4)$$

where, *L* and *y* are the useful life and the replacement number of a specified component. The penalty cost for shedd load can be calculated as follows:

$$Cost_{shedd} = LOEE \times C_{shedd} \quad (5)$$

In this equation, C_{shedd} shows the average of penalty cost to load curtailment (US$/kWh).

The objective function is defined as Eq. (6):

$$OF_{sizing} = Min\left\{\sum_i \sum_{j=1}^{R} NPC_{i.j} + \sum_{j=1}^{R} Cost_{shedd.j} + NPC_{Trans} + \sum_n NPC_{SA.n} + \sum_n NPC_{incentive.n} + \sum_{j=1}^{R} Cost_{buy.j} - \sum_{j=1}^{R} Cost_{sell.j}\right\} \quad (6)$$

where, *i* shows the components in smart MG, *R* is the project lifetime, NPC_{SA}, *n* specifies the net present value of the surplus investment cost of the nth smart components. $\sum NPC_{Trans}$ represents the net present cost value of the distribution transformer. $NPC_{incentive.n}$ determines the net present value of the nth smart appliances incentive, which can be calculated as below:

$$NPC_{incentive.n} = (Incentive\_avl_n + Incentive\_shift_n) \times PWA \quad (7)$$

where, $Incentive\_avl_n$ and $Incentive\_shift_n$ can be calculated by following equations:

$$Incentive\_avl_i = \frac{1}{5} \frac{SAC_i}{N\,(start-ave)_i} \times N\,(avl)_i \quad (8)$$

$$Incentive\_shift_i = \frac{SAC_i}{N\,(start-ave)_i} \times N\,(shift)_i \quad (9)$$

where, *SACi* is the surplus cost which should be paid for ith appliance (e.g., washing machine). $N\,(start-ave)_i$ determines the average usage number of ith smart appliance during one year. $N\,(avl)$ shows the number that ith appliance is available. It is considered in this study that smart appliances can receive incentive when they are available in specific hours, and $N\,(shift)_i$ specifies the shifting number of ith appliance annually.

$$Cost_{buy} = \sum_{t=1}^{8760} P_{buy}(t) \times Price_{buy}(t) \quad (10)$$

$$Cost_{sell} = \sum_{t=1}^{8760} P_{sell}(t) \times Price_{sell}(t) \quad (11)$$

where, $P_{buy}(t)$ and $P_{sell}(t)$ show the amount of power bought/sold from/to the network at *t*, while $Price_{buy}(t)$ and $Price_{sell}(t)$ determine the price of electricity bought or sold from/to distribution network per kWh at *t*.

In this situation, the surplus power is sold to the distribution network, and the shortages are bought from it.

The objective function should be optimized by considering following constraints:

$$E[ELF] \leq ELF_{max} \quad (12)$$
$$0 \leq N_i \quad (13)$$
$$0 \leq \theta_{PV} \leq {}^{\pi}/_{2} \quad (14)$$
$$E_{tank}(0) \leq E_{tank}(8760) \quad (15)$$
$$P_{sell}(t) \leq N_{TR}(max) \quad (16)$$
$$P_{buy}(t) \leq N_{TR}(max) \quad (17)$$

θ_{PV} is the installation angle of the PV array, and constraint (15) determines that the saved energy in tank should not be lower than the primary energy. This constraint guarantees that reliability calculations are performed for the worst condition. $N_{TR}(max)$ shows the maximum capacity of the distribution transformer.

$$ELF = \frac{1}{N}\sum_{t=1}^{N}\frac{Q(t)}{D(t)} \quad (18)$$

where, *Q(t)* shows the amount of load which is lost (is not supplied) (kWh), and *D(t)* shows the amount of demand (kWh). *ELF* is the equivalent loss Factor. Since *ELF* specifies more information about the amount of curtailment, it is applied as the main reliability index in this paper. The maximum acceptable amount for ELF is equal to 0.01 [29].

The renewable energy penetration percentage (REPP) can be determined by Eq. (19).

$$REPP = \frac{\sum_{t=1}^{8760}\frac{P_{REN-Direct}(t)}{P_{load}(t)}}{8760} \times 100 \quad (19)$$

where, $P_{REN\text{-}Direct}$ is the produced power of the RERs, which is directly specified to the users. The amounts of REPP in three studied MGs are presented in Table 1, which shows the high penetration of RERs in this study.

2.2. The optimal siting

The optimal placement of the RERs in suitable places in MG can decrease the amount of losses. Developing an appropriate method for optimal siting of RERs in the studied MG is necessary for reducing the amount of MG losses. In this section, the method is developed to minimize the cost during the assessment period (i.e., 20 years in this paper), by considering the effect of parameters like load growth.

In this section, the RERs are optimally placed in order to diminish the cost of the network during each year of the 20-year period. The optimal place of RERs is specified during each year of the 20-year period.

Table 1- *The amounts of REPP in three studied MGs*

Smart MG	REPP (%)
MG No.1	66
MG No.2	69
MG No.3	57

Although this paper does not discuss the protection subjects, it is considered in our problem definition. The unidirectional fault-current relay is considered in conventional grids, but applying them in microgrids may lead to mal functioning of the relays. As a result, bidirectional current relays should be applied in microgrids especially when the penetration of renewable energy systems is high. It is studied in [30] that applying DGs in microgrids causes bidirectional fault current which disturbs the function of conventional protection relays, and using bidirectional relays can be a solution for this problem.

As the reversal of current flow in microgrid distinguishes theses grids with simple radial distribution systems, the novel protection method should be applied in this case. Considering the sequence data in system applying bidirectional relays can be helpful in order to identify the fault truly. The directional over-current relay can be used in this study, which is considered the positive sequence and negative sequence currents in order to detect unbalanced and balanced fault [31].

The energy management system (EMS) is in communication with all of the RERs and protection devices. When a fault occurs, the EMS receives all information about DGs' state and protection devices. The directional over-current relays identify the direction of fault current, and the EMS identifies the location of fault by information received from relays.

It is considered that the movement of DGs will be possible if this component is applied during *MRT* period in the first place. For example, if the quantity of *MRT* is assumed two years, it means that the place of specified DG can be altered every two years. The amount of *MRT* is determined based on the technology of DG, mechanical difficulties and portable capability. A_{ija} is a binary variable that will be equal to 1 when ith DG is placed in location (a) at jth year, nevertheless it will be equal to 0.

MRT depends on two important parameters:

- DC_{iab} which is the movement cost of ith DG from place a to place b.
- $H_{i,trans}$ is the required time for movement of ith DG.

These two parameters especially the second one are dependent on the DG technology. Some technologies like MT, FC and PV require less time for movement. For example, transporting PV from place a to place b takes about one week, so $H_{i,trans}$ is equal to one week. Furthermore, their cost of movement is less in comparison with other technologies. In this study, it is assumed that these technologies can be moved. On the contrary, other technologies like WT cannot be moved due to the long time and the high cost of dismantling of WT.

The objective function minimizes the losses and the costs of movement of DGs. In the studied MG, WTs, PVs, FC and MT are taken into account, which are divided into two groups:

- 1st type: DGs only inject active power: PVs and FC.

- 2nd type: DGs produce active power with constant power factor: WTs and MT.

2.2.1. *The network losses:* The network loss is annually calculated based on Eq. (20) [32]:

$$P_{loss} + jQ_{loss} = \sum_{j=1}^{N_{bus}} \sum_{t=1}^{8760} V_j(t) \cdot I_j^*(t) \quad (20)$$

where, $V_j(t)$ and $I_j(t)$ show the voltage and current of bus j at t, and P_{loss} and Q_{loss} denote the active and reactive power loss. The injected power is defined by the difference between the produced and consumed power:

$$P_j(t) = P_{DGj}(t) - P_{Dj}(t) \quad (21)$$

$$Q_j(t) = Q_{DGj}(t) - Q_{Dj}(t) \quad (22)$$

$P_{Dj}(t)$ and $P_{DGj}(t)$ are the active power consumed and produced respectively in jth bus at t. Similarly, $Q_{DGj}(t)$ and $Q_{Dj}(t)$ denote the reactive power.

$$P_{loss} = \sum_{i=1}^{N_{bus}} \sum_{j=1}^{N_{bus}} \sum_{t=1}^{8760} \Big[\alpha_{ij}^p \Big(\big(P_{DGi}(t) - P_{Di}(t)\big)\Big)\Big(P_{DGj}(t) - P_{Dj}(t)\Big) + (Q_{DGi}(t) - Q_{Di}(t))(Q_{DGj}(t) - Q_{Dj}(t))\Big) + \beta_{ij}^p\big(\big(Q_{DGi}(t) - Q_{Di}(t)\big)\Big(P_{DGj}(t) - P_{Dj}(t)\Big) - (P_{DGi}(t) - P_{Di}(t))(Q_{DGj}(t) - Q_{Dj}(t))\big)\Big] \quad (23)$$

The reactive power is calculated as follows for WT and MT considering their constant power factor.

$$Q_{DG}(t) = P_{DG} \tan(arccos(PF)) \quad (24)$$

In order to calculate the loss, the bus angle and voltage should be determined by the load flow. In this study, load flow is carried out by DIgSILENT power factory software.

2.2.2. The cost of DGs movement:

The cost related to DGs movement is included two different parts:

- The cost of DGs movement (DC_{iab})
- The cost of lost energy in this period (LDG_{ij})

The total cost of movement (TC_{ij}) includes the cost of changing location ith DG (DC_{iab}) from location (a) at (j-1)th year to location (b) at (j)th year and the cost of lost energy (LDG_{ij}).

DC_{iab} contains the cost of transporting ith DG from the primary place (a) through different routes and the cost of preparing a new place (b) in addition to installation cost. In this study, the expense of installation and preparing in a new place is assumed 20% of initial DG cost. The transporting cost of DG depends on the DG weight and the length of the path.

The total cost of movement is calculated as follows:

$$TC_{ij} = \sum_{a=1}^{N_{bus}} \sum_{b=1}^{N_{bus}} ((A_{i.j-1.a} \times A_{i.j.b}) \times (DC_{iab} + LDG_{ij})) \quad (25)$$

$$LDG_{ij} = h_{i.trans} \times G_{i.rated} \times EP_j \quad (26)$$

where, DC_{iab} is the transportation cost of ith DG from location (a) to location (b), $h_{i.trans}$ shows the required time for transporting ith DG, EP_j specifies the price of buying energy at jth year from distribution grid, and $G_{i.rated}$ determines the rated power of ith DG.

To reach this point, the objective function of optimal DG placing in smart MG is defined as below:

$$OF_{siting} = Min\Big(\sum_{i=1}^{N_{DG}} \sum_{j=1}^{R} \sum_{a=1}^{N_{bus}} \big[\big(P_{loss.j} \times A_{ija} \times penalty\big) + \big(TC_{ij} \times A_{ija}\big)\big]\Big) \quad (27)$$

where, R is the number assessment years (20 years in this paper), N_{bus} shows the possible places for installation of DG and N_{DG} determines the number of DG types.

The constraints of this objective function are as follows:

$$|V|_i^{min} \le |V_i| \le |V|_i^{max} \quad (28)$$

$$\delta_i^{min} \le \delta_i \le \delta_i^{max} \quad (29)$$

$$I_{line} \le I_{line}^{max} \quad (30)$$

where constraint (28) is related to voltage limitations, inequality (29) shows the allowable angle deviations based on voltage stability, and constraint (30) determines the maximum allowable loading current and thermal limitations. It is also assumed that changing the location of WT is not possible, but PVs, FC and MT can be moved every 3 years.

Since the objective of this paper is to determine the optimal place and size simultaneously, the objective function is defined as below.

$$OF = min_x\{OF_{sizing} + OF_{siting}\} \quad (31)$$

where, X is the vector including the optimization variables (optimal place and size). The constraints of this objective function are presented in (12)-(17) and (28)-(30).

The general flowchart for MGs which do not participate in a competitive market is presented in Figure 1. In this study, Particle swarm optimization (PSO) method is applied, and its parameters are presented in Table 2.

The general flowchart for optimal sizing and siting during one year is shown in Figure 2.

Phase 2 in Ekbatan residential complex is being developed now, so two types of load growth are considered in this paper. The first type is related to No. 1-8 buses in phase 2, and the second type is related to other buses.

The general flowchart for determining the steps for sizing and siting of RERs applying PSO algorithm is presented in Fig. 3. The amount of peak load at j year is calculated as follows:

$$LP_j = LP_0(1 + a)^{j-1} \quad (32)$$

where, a is the load growth rate, LP_0 shows the initial peak load, and LP_j determines the peak load at jth year. The impact of this load growth in the determination of optimal location and size is considered. The added components at ith year in smart MG produce power during (N_{year}-i+1) years. The optimization is annually performed to extract the optimal size and site considering load growth.

Table 2- *PSO parameters*

Inertia (w)	C2	C1	Number of iterations	Population
0.7	2	2	200	30

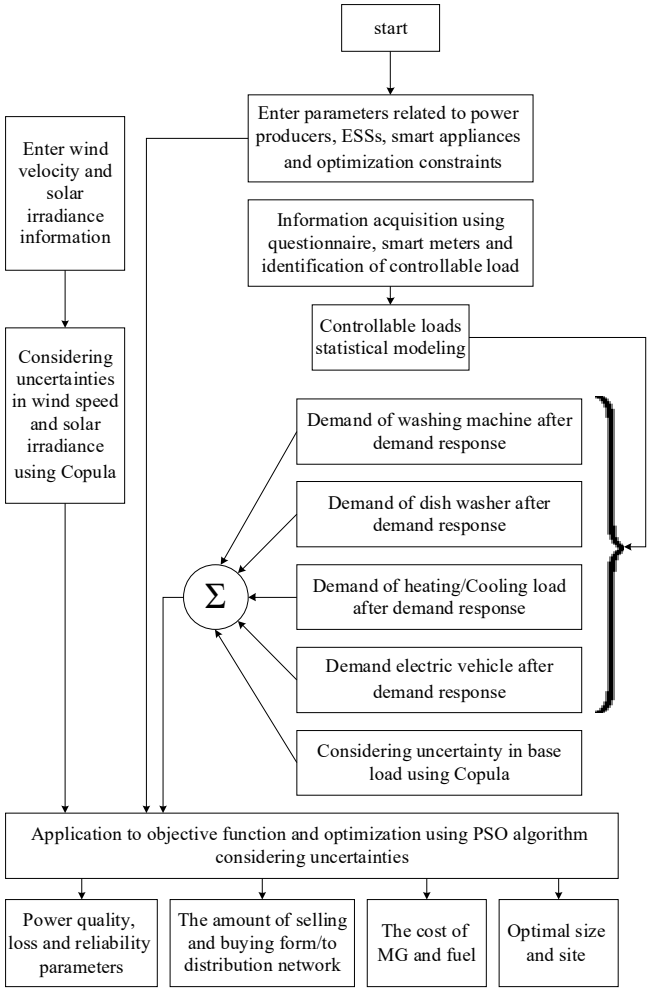

Fig. 1. *The main flowchart for proposed method*

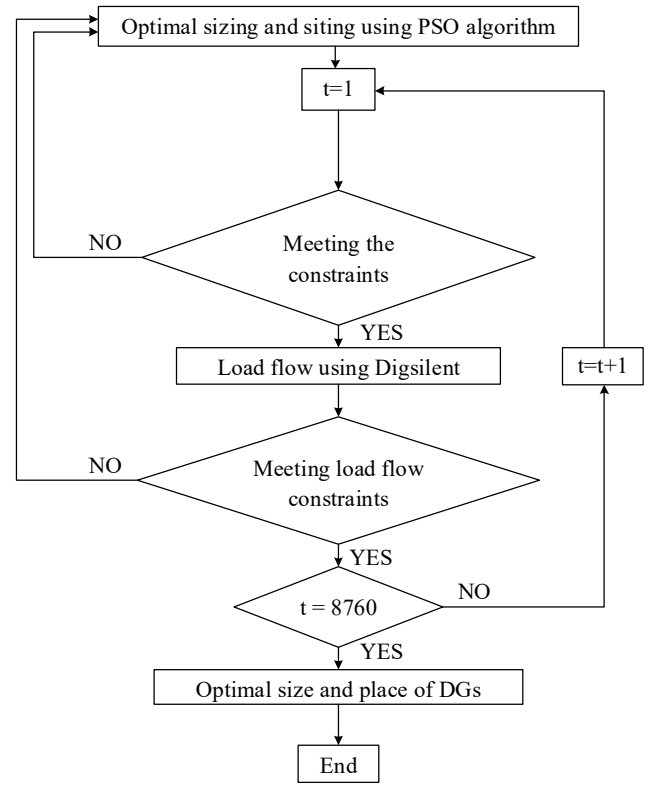

Fig. 2. *The main flowchart for optimal sizing and siting during one year*

The price of RERs are decreasing during time considering technology development [33], so one of the novelties in this section is taking into account the investment cost of RERs in the year of installation. For example, if there is a need to add PV at 5th year of study to the system, the forecasted investment cost at 5th year is considered in calculations. As a result, the results are closer to the real situation.

Different reasons including the reduction in labour and material, competition in the global market, increasing capacity factor and decreasing installed cost, reducing O&M cost are mentioned for this price decrease [33].

The investment costs of RERs in the period between 2010 and 2016 are presented in this report. In order to consider inflation in comparing prices in different years, all costs are presented in real 2016 USD. All prices are considered in 2016 USD value, so they can be compared together. The real data is used in this report in order to show the decreasing trend of RERs' costs, which is used in our study. In [34], the amount of decrease in the legalized cost of energy for residential PV is forecasted 67% by 2030. The average worldwide inflation rate in the period between 2012 and 2017 is announced 4.07% and 3.2% respectively [35], so the amount of inflation in next years is estimated based on these quantities, which are used in RERs' price projection.

3. Simulation and result discussion

The Ekbatan residential complex is considered as the research case study. Ekbatan has three separate sets of buildings called respectively phase 1, 2 and 3 considered as smart microgrids. Although there is no electrical connection between them, each of these phases is connected to 63/20 kV substation by a 20 kV cable. The underground 20 kV cables are applied in distribution grid in Ekbatan complex. The schematic of this MG is depicted in Fig. 4. To reach this point, the electricity tariff in Iran is used. The off-peak rate is equal to 0.1 $/kWh while the peak rate is equal to 0.15 $/kWh.

The smart microgrid No. 1 consists of WT, PV panel, fuel cell, electrolyzer, hydrogen tank, controllable loads (washing machine, dishwasher, heating/cooling system and plug-in electric vehicles) and uncontrollable loads. The line data for this MG is presented in Table 3. The schematic of MG No. 1 and the single-line diagram of MG No.1 are represented in Figures 5 and 6.

Generation components in smart microgrid No. 2 are WT, PV panel, and battery. Similar to the first smart microgrid, the controllable loads are washing machine, dishwasher, heating/cooling system and plug-in electric vehicles, and its line data is presented in Table 4. The schematic of MG No. 2 and the single-line diagram of MG No.2 are shown in Figures 7 and 8.

Table 3- *The line data for smart MG 1*

First bus	Second bus	Resistance (pu)	Reactance (pu)
A1	A2	0.0058	0.0029
A2	A3	0.0308	0.0157
A2	A4	0.0102	0.0098
A4	A5	0.0939	0.0846
A5	B1	0.0255	0.0298
B1	B2	0.0442	0.0585
A3	B3	0.0282	0.0192
B3	B4	0.0560	0.0442
B4	C2	0.0559	0.0437

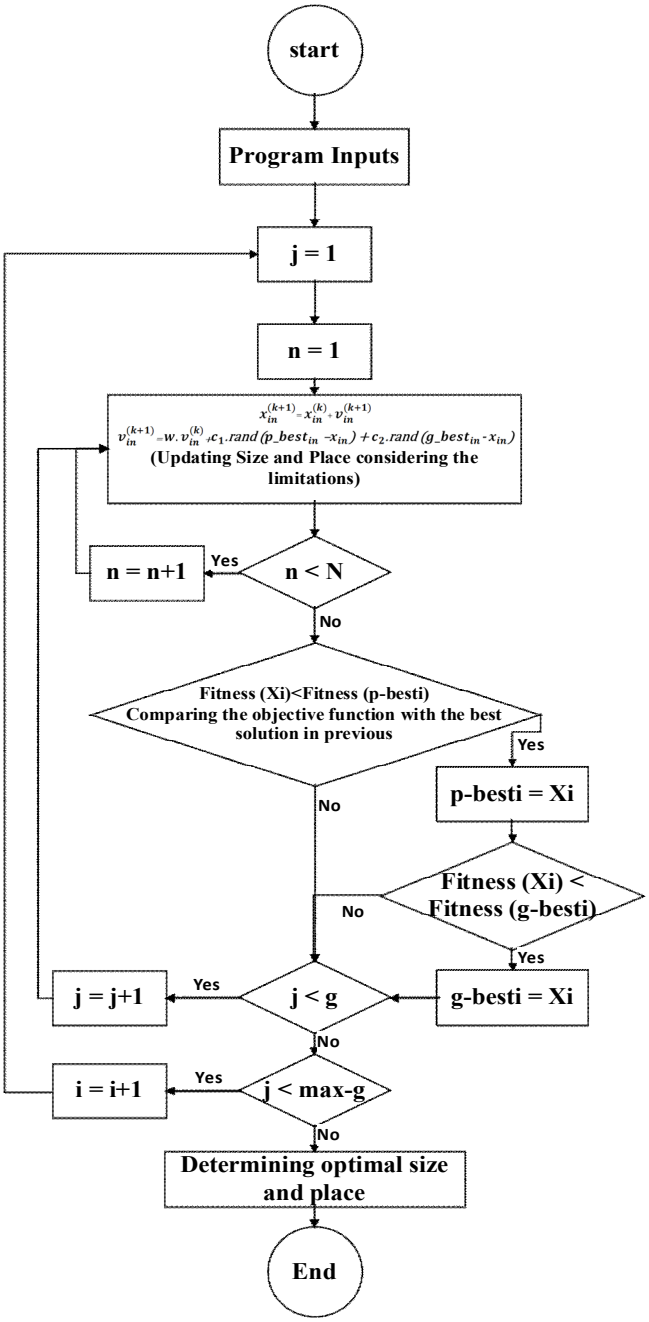

Fig. 3. *The general flowchart for determining the steps for sizing and siting of RERs*

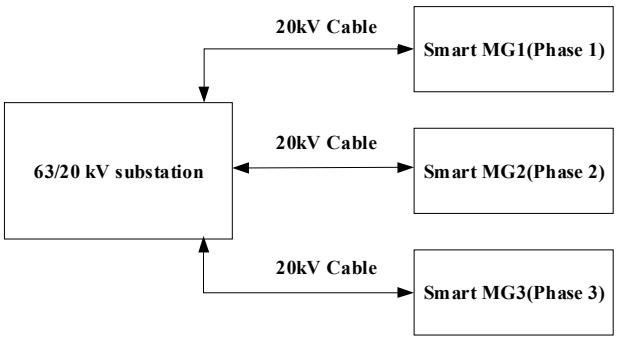

Fig. 4. *Schematic of MG*

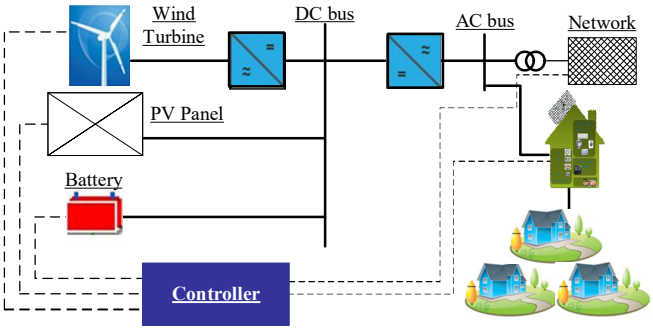

Fig. 5. *Schematic of MG No. 1*

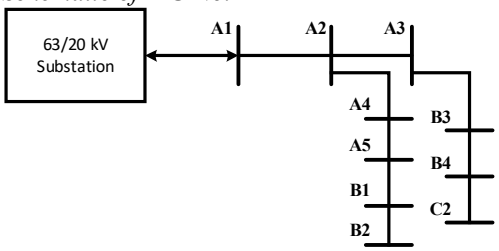

Fig. 6. *Single-line diagram of MG No. 1*

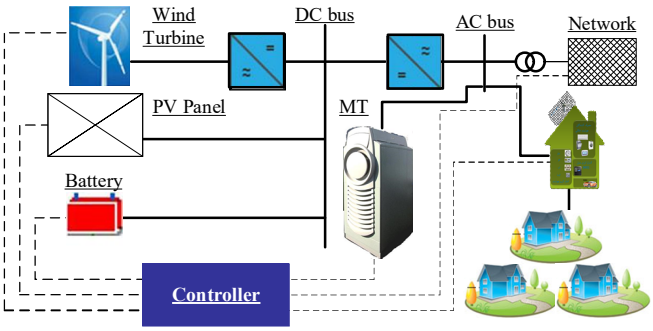

Fig. 7. *Schematic of MG No. 2*

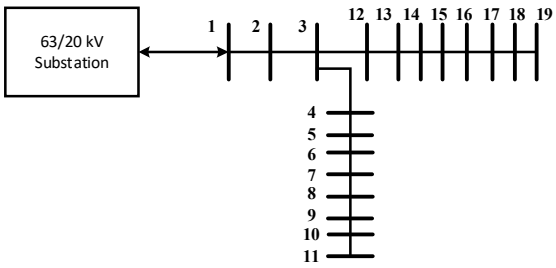

Fig. 8. *Single-line diagram of MG No. 2*

Table 4- *The line data for smart MG 2*

First bus	Second bus	Resistance (pu)	Reactance (pu)
1	2	0.0238	0.0121
2	3	0.0511	0.0441
3	12	0.0117	0.0386
12	13	0.1068	0.0771
13	14	0.0643	0.0462
14	15	0.0651	0.0462
15	16	0.0123	0.0041
16	17	0.0234	0.0077
17	18	0.0916	0.0721
18	19	0.0338	0.0445
3	4	0.0127	0.0065
4	5	0.0559	0.0437
5	6	0.0502	0.0437
6	7	0.0317	0.0161
7	8	0.0608	0.0601
9	10	0.0194	0.0226
10	11	0.0213	0.0331

Table 5- *The line data for smart MG 3*

First bus	Second bus	Resistance (pu)	Reactance (pu)
D1	D2	0.0466	0.0340
D2	E1	0.0804	0.1074
E1	E2	0.0457	0.0358

WTs, PV panels, micro turbines and battery are generation components in smart grid No. 3. The controllable loads of smart microgrid No. 3 are like smart microgrids No. 1 and No. 2. The parking lot of each MG is located at that bus in these three smart microgrids. Furthermore, the charge/discharge management of plug-in electric vehicles has effects only on that bus. The schematic of MG No. 3 and the single-line diagram of MG No.3 are represented in Figures 9 and 10.

Every bus in Ekbatan complex includes some houses, which is specified in Table 6. The charge/discharge management of the plug-in electric vehicles cost is considered in Eq. (6). The effect of the charge/discharge management of the plug-in electric vehicles is also considered in the annual normalized load curve because the load is determined considering the electric vehicle required power consumption.

The assumed constraints in charge/discharge management are as bellow:

- Complete charge at exit time of parking,
- Number of electric vehicles in the parking,
- Limitations in charge/discharge times in batteries,
- Battery power level and capacity.

The total MG's load after electric vehicle management is shown in Fig. 13. When the produced power of RERs is more than loads, the electric vehicles are charged. Electric vehicles can be discharged in a condition that the produced power of RERs is less than loads. In our study, the main aim of demand response is to utilize the RERs' production as much as possible, so when the production of RERs is higher than loads in microgrids, the electric vehicles are charged. This issue leads to a decrease in the energy bought from the main grid, so the cost of buying energy reduces. In fact, the maximum usage of surplus energy of RERs in order to charge electric vehicles is considered in our study, which causes a decrease in the bought energy from the main grid.

The peak demand in different buses in Ekbatan complex is presented in Table 6 without considering controllable loads.

In this section, the optimal sizing and siting for assumed smart MGs are carried out by the proposed method, and the PSO method is applied for optimization. To reach this point, the software developed in Matlab. The information related to annual solar irradiance and wind speeds are hourly extracted for Ekbatan complex (Figures 11 and 12). The load profile of Ekbatan complex is obtained from the distribution company. The uncertainty of sunlight, wind speed and load profile are considered by Copula method which is explained in the appendix, and the normalized diagram of sunlight, wind speed and load are hourly depicted on figures. The base load specification is extracted from the IEEE standard [36]. Table 6 determines the program inputs, and the nominal amounts are presented in Table 9. The expense of load curtailment in base load is considered 5.6 US$/kWh.

Table 6- *The specifications of houses and buses in Ekbatan complex*

Phase	Number of houses	Bus	Peak load (kW)
1	517	A1	500
1	532	A2	500
1	532	A3	500
1	532	A4	500
1	532	A5	500
1	613	B1	600
1	613	B2	600
1	613	B3	600
1	613	B4	600
1	514	C2	500
2	340	1	300
2	422	2	400
2	402	3	400
2	460	4	500
2	516	5	500
2	360	6	400
2	506	7	500
2	506	8	500
2	422	9	400
2	360	10	400
2	458	11	400
2	298	12	300
2	506	13	500
2	500	14	500
2	342	15	300
2	337	16	300
2	312	17	300
2	597	18	600
2	334	19	300
3	598	D1	600
3	598	D2	600
3	445	E1	400
3	445	E2	400

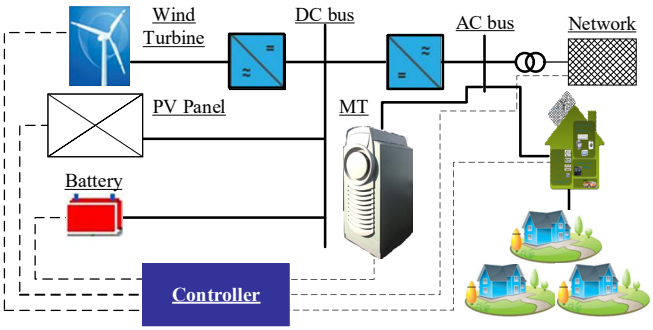

Fig. 9. *Schematic of MG No. 3*

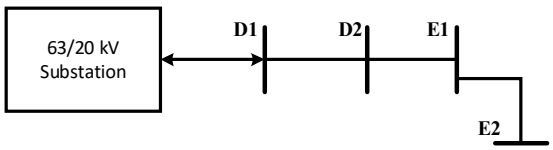

Fig. 10. *Single-line diagram of MG No. 3*

For instance, the results of optimal location and size are presented in Table 8 and Figs. 14 to 20 for smart MGs. In Table 8, N_{Wind} is the optimal number of WTs, N_{PV} shows the optimal number of PVs, N_{MT} specifies the optimal size of MT, N_{bat} determines the optimal size of battery, and B_{PV}, B_{Wind}, B_{MT} and B_{Bat} are respectively optimal place (No. of bus) of PV, WTs, MTs and batteries. In Table 10, the reliability indices are introduced, and it should be notified that DR and load growth are not considered in this case.

Table 7- *The program inputs*

Component	Initial cost ($/unit)	Replacement cost ($/unit)	Annual O&M cost ($/unit-year)	Useful life	Efficiency	Availability
WT (50 kW)	75000	40000	750	20	-	96
PV (1 kW)	2000	1500	20	20	-	96
Electrolyzer (1 kW)	2000	1500	25	20	75	100
Hydrogen tank (1 kg)	1300	1200	15	20	95	100
Fuel cell (1 kW)	3000	2500	175	5	50	100
Inverter DC/AC (1 kW)	800	750	8	15	90	98/99
MT (1 kW)	400	340	20	5	30	100
Battery (1 kW)	500	400	25	3	85	100

Table 8- *The optimal size and location of components smart microgrids*

	N_{Wind}	N_{PV}	N_{bat}	N_{MT}	N_{FC}	M_{tank}	B_{PV}	B_{Wind}	B_{MT}	B_{Bat}	B_{FC}	MG cost ($)
MG No. 1	265	9886	-	-	2150	29975	A2	B1	-	-	B4	14.8526×10^7
MG No.2	252	14210	22340	-	-	-	10	18	-	3	-	19.8249×10^7
MG No. 3	87	3780	10500	2050	-	-	E2	E2	D2	E2	-	8.1777×10^7

As it can be seen from normalized load curve Fig. 13, the peak load has occurred in the hours 2000th -3000th and 6000th- 7000th. The study of determining optimal size and place is done hourly during one year period, so the peak hours refer to the annual peak. This curve is calculated based on the residential IEEE P.U. [37]. The base for the per-unit values is the sum of all peak load which is presented in Table 6, and it is equal to 15200 kW.

The loading current for lines D2-E1 and E1-E2 are shown in Figures 15 and 16. The amount of line current should be lower than the specified amount according to Eq. (29) (in this paper, $I_{line}^{max} = 1.05 \times I(P \cdot U)$), and this constraint is fulfilled. The maximum current has occurred at hours when the loads are in their maximum level.

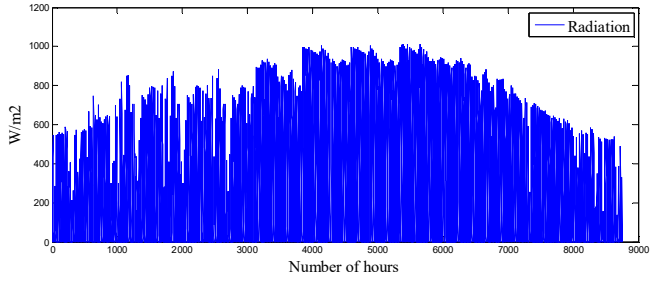

Fig. 11. *The annual sunlight in Ekbatan complex*

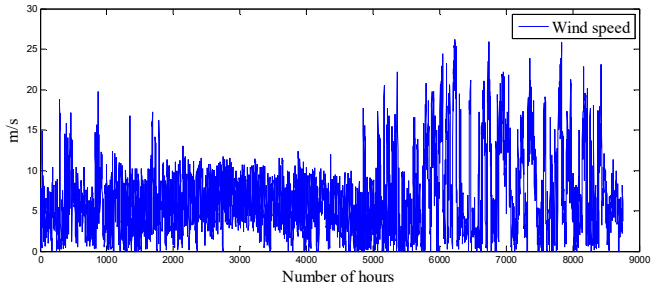

Fig. 12. *The annual wind speed in Ekbatan complex*

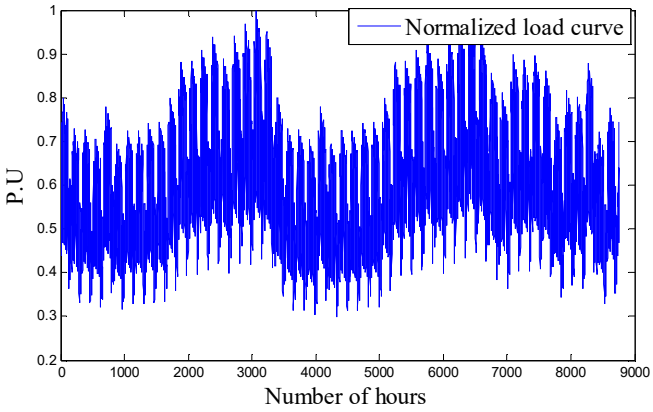

Fig. 13. *The annual normalized load curve*

Table 9- *The nominal amounts*

	Input	Quantity
1	Fuel cost ($/Mbtu)	0.12
2	Inflation rate	0.06
3	Project life (year)	20
4	Population	30
5	Iteration	200
6	ELF_{max}	0.01

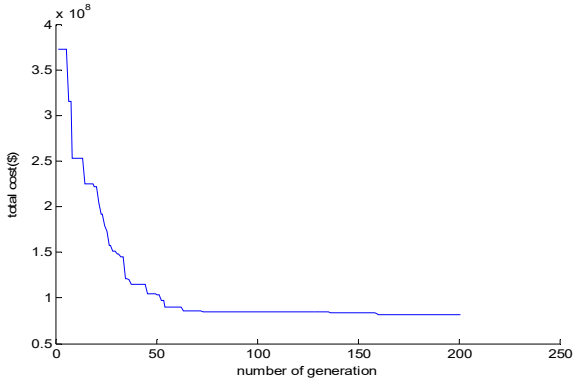

Fig. 14. *Convergence curve of PSO algorithm*

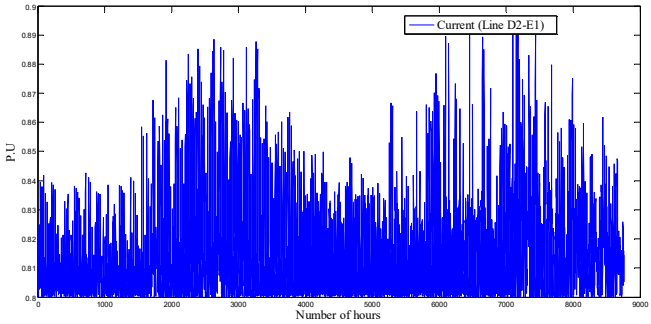

Fig. 15. *Loading line current between D2 and E1 bus*

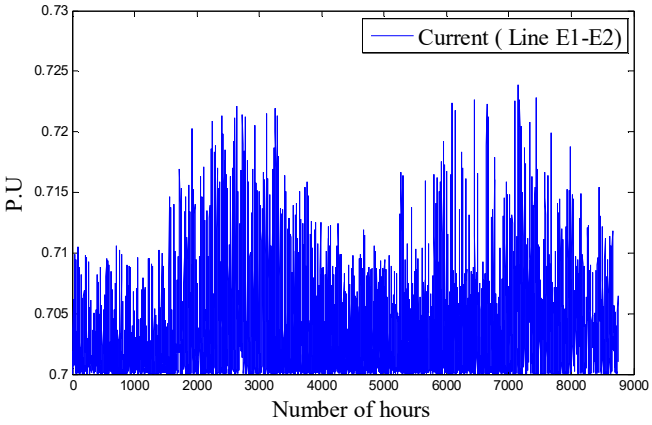

Fig. 16. *Loading line current between E1 and E2 buses*

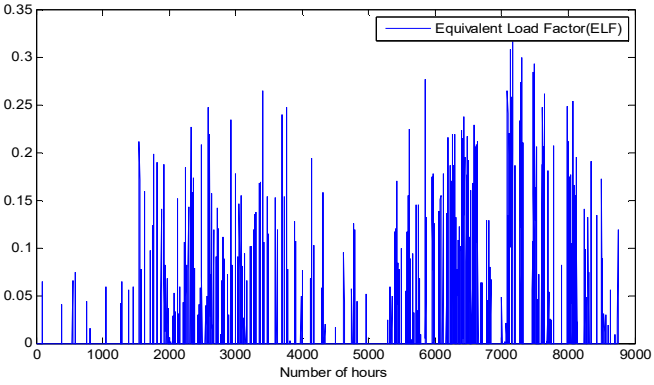

Fig. 17. *hourly equivalent loss factor*

Figure 17 illustrates MG No. 3 ELF. Since the peak load is at 2000th-3000th hour, and the wind speed is low in this hour, the ELF is considerable in this period. The same situation has occurred for 6000th-7000th hours. In other words, the amount of loss in this period increases. The voltage profile at bus D1 is shown in Fig. 18. As this bus is connected to the distribution network, it is considered as the infinite bus.

$$0.95|V_i| \leq |V_i| \leq 1.05|V_i| \qquad (33)$$

The voltage profile at buses D2, E1 and E2 are shown in Figures 18-20, and their modifications are in allowable range. In this study, the voltage constraint is defined as follows, and the minimum voltage has occurred at peak hours.

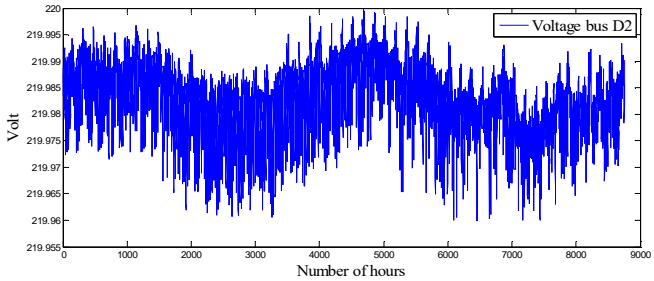

Fig. 18. *Voltage at bus D2*

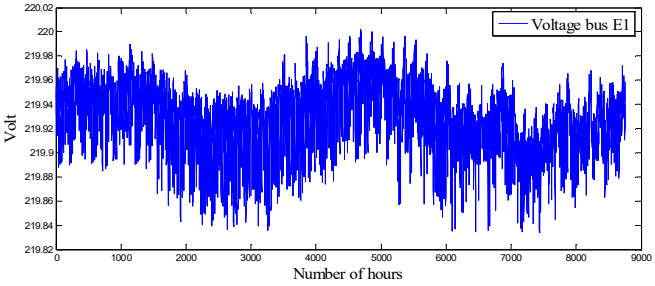

Fig. 19. *Voltage at bus E1*

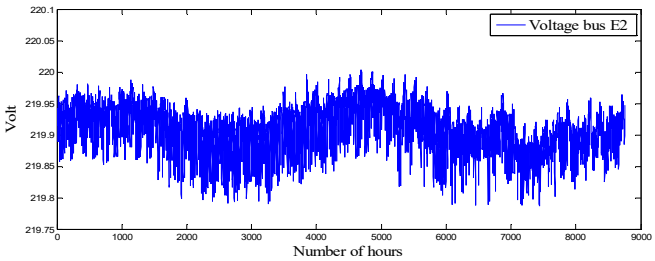

Fig. 20. *Voltage at bus E2*

Table 10- *The optimal size and the annual surplus cost for MG No. 1*

Year	Load growth (kW)	WT	PV	Electrolyzer	Hydrogen tank	FC	ELF × 10^{-3}	Cost ($)
1	0	265	9886	23879	29975	2150	10	14.8526×10^7
2	108	5	189	450	575	44	10	0.257052×10^7
3	218	8	386	976	1210	82	10	0.512105×10^7
4	330	14	543	1342	1781	131	10	0.8076589×10^7
5	445	21	810	1867	2370	177	10	1.123964×10^7
6	562	27	1020	2480	3019	223	0	1.445771×10^7
7	681	32	1239	3005	3615	270	10	1.773089×10^7
8	802	38	1472	3562	4532	317	8.2815	2.105886×10^7
9	926	44	1689	4032	5140	370	10	2.456987×10^7
10	1053	50	1921	4657	5845	417	10	2.797453×10^7

3.1. The impact of load growth on optimal sizing and siting

The 1-8 buses in Ekbatan complex are being developed but there is no development in other buses. Furthermore, there are two types of load growth in this study. The first model is related to buses 1-8 (6%), and the second model is related to other buses (2%). The peak load is calculated by equation 80-4. It is assumed that the load growth is saturated after 10 years [36].

The load growth has occurred every year comparing to previous year, hence new components should be added to MG in each year. The added components at ith year will produce power for (R-i+1) years (R shows the project life). The total investment cost at the beginning of the project is calculated as follows:

$$NPC_{add-units} = \frac{NPC_{unit-year(i)}}{(1+i_r)^{i-1}} \quad (33)$$

The optimal location of smart MG No. 1 is presented in Table 11. In Table 12, the optimal size for MG No. 1 and the annual surplus cost is determined. The optimal locations of smart MG No. 2 and No. 3 are presented in Tables 13-14, respectively.

As it is shown in Tables 11 and 14, the optimal place of smart appliances in MG has not changed by load growth because of same load growth in all buses. In the MG No. 2, since buses 1-8 are being developed, and load growth is more in these buses, PV is transferred to bus 7 at 5th year. Although the movement of WT is impossible, other appliances can be moved every 3 years.

Table 11- *Reliability indices for MG No. 3*

ELF	*LOEE* (MWh/yr)	*LPSP*	*LOLE* (hr/yr)
0.00836	57.3726	0.008815	2.96

Table 12- *The optimal location of components in smart MG No. 1*

Year	Location of WT	Location of PV	Location of FC (electrolyzer and Hydrogen tank)
1	A2	B1	B4
2	A2	B1	B4
3	A2	B1	B4
4	A2	B1	B4
5	A2	B1	B4
6	A2	B1	B4
7	A2	B1	B4
8	A2	B1	B4
9	A2	B1	B4
10	A2	B1	B4

Table 13- *The optimal location of components in smart MG No. 2*

Year	Location of WT	Location of PV	Location of BT
1	18	10	3
2	18	10	3
3	18	10	3
4	18	10	3
5	18	7	3
6	18	7	3
7	18	7	3
8	18	7	3
9	18	7	3
10	18	7	3

Table 14- *The optimal location of components in smart MG No. 3*

Year	Location of WT	Location of PV	Location of MT
1	E2	E2	D2
2	E2	E2	D2
3	E2	E2	D2
4	E2	E2	D2
5	E2	E2	D2
6	E2	E2	D2
7	E2	E2	D2
8	E2	E2	D2
9	E2	E2	D2
10	E2	E2	D2

4. Conclusion

In this paper, the optimal place and size of WT, PV, FC, electrolyzer and hydrogen tank were determined in a smart MG. On a case study, the result showed that the proposed algorithm based on PSO could optimally find the capacity and location of REs and storages, and its efficiency on mitigating the total cost along with improved reliability was proved. The proposed methodology was applied on three different MGs, and optimal place and size of their RERs and ESSs were specified. The impact of 2% load growth was studied in MG including WT/PV/FC/Hydrogen tank/battery. The load growth of 108 kW in the MG at 1st year of study led to only 2% increase in the total cost. Furthermore, the effect of different load growth (i.e., 6% only for some buses of another MG including PV/WT/battery) was investigated in this paper. The proposed method was applied for WT/PV/FC/hydrogen tank hybrid system, which is already one of the most complex systems, but this method can be applied for siting and sizing of other cases too.

Acknowledgments

Authors would like to thank the research council of Islamic Azad University, Damavand, Iran for financial support of this research project.

Appendix

The Copula method is the function that connects the multivariable probability density function to the one variable density function. The mathematical definition of the Copula is as follows [38].

$$\boldsymbol{C[F_1(x_1), F_2(x_2), \dots, F_n(x_n)] = F(x_1, x_2, \dots, x_n)} \quad \boldsymbol{(34)}$$

The copula method converts different one variable probability density functions to the one multivariable density function [39]. In order to use the Copula method for wind and solar irradiance, the next steps should be applied:

1) Enter the sample information in the matrix in a condition that the columns are the information for every hour (nv = 24), and each row is related to the one day in a year (ns = 365).
2) Each column should be modeled with a suitable probability density function. One of the unique

advantages of the Copula method is that it can use different probability density functions.

3) Calculation of the correlation matrix between different probability density functions
4) Applying the Copula method
5) Acquiring required information in the defined period

After applying these steps, the probability density function for wind and solar irradiance is determined. In our study, the real data of hourly variation of solar irradiation level and wind speed over the year are extracted using two different sensors. A wind speed sensor (Si-RS485TC-2T-v) and digital silicon irradiance (Si-RS485TC-T) are applied in order to gather wind speed and irradiance data over the year. The irradiance and wind speed data for Ekbatan complex are shown in Fig.13 and Fig.14 respectively.

References

[1] S. D. Clercq, B. Zwaenepoel and L. Vandevelde, "Optimal sizing of an industrial microgrid considering socio-organisational aspects," IET, vol. 12, no. 14, pp. 3442-3451, 2018.

[2] S. M. o. W. G. f. o. e. s. sizing, "Hamed valizadeh haghi; Saeed lotfifard," *IEEE transactions on sustainable energy,* vol. 6, no. 1, pp. 113-121, 2015.

[3] H. Xing, H. Fan, X. Sun, S. Hong and H. Cheng, "Optimal Siting and Sizing of Distributed Renewable energy in an active distribution network," *CSEE journal of power and energy systems,* vol. 4, no. 3, pp. 380-387, 2018.

[4] S. Saha and V. Mukherjee, "optimal placement and sizing of DGs in RDS using chaos embedded SOS algorithm," *IET,* vol. 10, no. 14, pp. 3671-3680, 2016.

[5] N. Kanwar, N. Gupta, K. R. Niazi and A. Swarnkar, "optimal distributed resource planning for microgrids under uncertain enviornment," *IET,* vol. 12, no. 2, pp. 244-251, 2018.

[6] Y. Y. Zhao, Y. R. An and Q. Ai, "research on size and location of distributed generation with vulnerable node identification in the active distribution network," *IET,* vol. 8, no. 11, pp. 1801-1809, 2014.

[7] L. Yu, D. Shi, X. Guo, Z. Jiang, G. Xu, G. Jian, J. Lei and C. Jing, "An Efficient Substation Placement and Sizing strategy based on GIS using semi-supervised learning," *CSEE journal of power and energy systems,* vol. 4, no. 3, pp. 371-379, 2018.

[8] U. Akram, M. Khalid and S. Shafiq, "Optimal sizing of a wind/solar/battery hybrid grid-connected microgrid system," *IET renewable power generation,* vol. 12, no. 1, pp. 72-80, 2018.

[9] S. Ahmadi and S. Abdi, "Application of hybrid big bang-big crunch algorithm for optimal sizing of stand-alone hybrid PV/wind/battery system," Solar energy, vol. 134, pp. 366-374, 2016.

[10] A. Ogunjuyigbe, T. Ayodele and O. Akinola, "Optimal allocation and sizing of PV/wind/split-diesel/battery hybrid energy system for minimizing life cycle cost, emission and dump energy of remote residential building," *Applied energy,* vol. 171, pp. 153-171, 2016.

[11] C. Lai and M. Mcculloch, "Sizing of stand-alone solar PV and storage system with anaerobic digestion biogas power plants," *IEEE Transactions on Industrial Electronics,* vol. 64, no. 3, pp. 2112-2121, 2017.

[12] A. Askarzadeh, "A novel solution for sizing a photovoltaic/diesel HPGS for isolated sites," *IET renewable power generation,* vol. 11, no. 1, pp. 143-151, 2017.

[13] A. S. A. Awed, T. H. M. EL-Fouly and M. M. A. Salama, "Optimal ESS Allocation for Benefit Maximization in distribution networks," *IEEE transactions on smart grid,* vol. 8, no. 4, pp. 1668-1678, 2017.

[14] I. S. Bayram, M. Abdallah, A. Tajer and K. A. Qaraqe, "A Stochastic Sizing Approach for Sharing-Based energy storage applications," *IEEE transactions on smart grid,* vol. 8, no. 3, pp. 1075-1084, 2017.

[15] R. Fernandez-Blanco, Y. Dvorkin, B. Xu, Y. Wang and D. S. Kirschen, "Optimal Energy Storage Siting and Sizing: A WECC case study," *IEEE transactions on sustainable energy,* vol. 8, no. 2, pp. 733-743, 2017.

[16] H. Bakhtiari and R. A. Naghizadeh, "Multi-criteria optimal sizing of hybrid renewable energy systems including wind, photovoltaic, battery, and hydrogen storage with E-constraint method," *IET renewable power generation,* vol. 12, no. 8, pp. 883-892, 2018.

[17] J. Mahmodimehr and M. Shabani, "Optimal design of hybrid photovoltaic-hydroelectric standalone energy system for north and south of Iran," *Renewable energy,* vol. 115, no. 1, pp. 238-251, 2018.

[18] L. Ferrari, A. Bianchini and G. Galli, "Influence of actual component characteristics on the optimal energy mix of a photovoltaic-wind-diesel hybrid system for a remote off-grid application," *Journal of cleaner production,* vol. 178, pp. 206-219, 2018.

[19] S. Singh and E. Fernandez, "Modeling size optimization and sensitivity analysis of a remote hybrid renewable energy system," *Energy,* vol. 143, pp. 719-731, 2018.

[20] Z. Shi, R. Wang and T. Zhang, "Multi-objective optimal design of hybrid renewable energy systems using preference-inspired coevolutionary approach," *Solar energy,* vol. 118, pp. 96-106, 2015.

[21] O. Erdinc, A. Tascikaraoglu, N. G. Paterakis, I. Dursun, M. C. Sinim and J. P. S. Catalao, "Comprehensive Optimization Model for Sizing and siting of DG units, EV charging stations, and energy storage systems," *IEEE transaction on smart grid,* vol. 9, no. 4, pp. 3871-3882, 2017.

[22] T. M. Masaud, O. Oyebanjo and P. Sen, "Sizing of large-scale battery storage for off-grid wind power plant considering a flexible wind supply-demand balance," *IET renewable power generation,* vol. 11, no. 13, pp. 1625-1632, 2017.

[23] J. Zhu, W. Gu, G. Lou, L. Wang, B. Xu, M. Wu and W. Sheng, "Learning Automata Based Methodology for Optimal Allocation of Renewable Distributed Generation Considering Network Reconfiguration," *IEEE access,* vol. 5, pp. 14275-14288, 2017.

[24] S. Shojaabadi, S. Abapour, M. Abapour and A. Nahavandi, "Optimal planning of plug-in hybrid electric vehicle charging station in distribution network considering demand response programs and

uncertainties," IET Generation, Transmission & Distribution, vol. 10, no. 3, pp. 3330-3340, 2016.
[25] H. Simorgh, H. Doagou-Mojarrad, H. Razmi and G. B. Gharehpetian, "Cost-based optimal siting and sizing of electric vehicle charging stations considering demand response programmes," IET Generation, Transmission & Distribution, vol. 12, no. 8, pp. 1712-1720, 2018.
[26] A. Chauhan and R. P. Saini, "Size optimization and demand response of a stand-alone integrated renewable energy system," Energy, vol. 124, pp. 59-73, 2017.
[27] S. Semaoui, A. Arab, S. Bacha and B. Azoui, "The new strategy of energy management for a photovoltaic system without extra intended for remote-housing," Solar energy, vol. 94, pp. 71-85, 2013.
[28] D. B. Richardson and L. D. Harvey, "Optimizing renewable energy, demand response and energy storage to replace conventional fuels in Ontario, Canada," Energy, vol. 93, pp. 1447-1455, 2015.
[29] R. Garcia and D. Weisser, "A wind-diesel system with hydrogen storage joint optimisation of design and dispatch," Renewable Energy, vol. 31, pp. 2296-2320, 2006.
[30] H. Laaksonen, "Protection principles for future Microgrids," *IEEE transaction on power electronics,* vol. 25, no. 12, pp. 2910-2918, 2010.
[31] D.-G. Jin, J.-C. Choi, D.-J. Won, H.-J. Lee, W.-k. Chae and J.-S. Park, "A Practical Protection Coordination Strategy Applied to Secobdary and Facility Microgrids," *Energies,* vol. 5, no. 12, pp. 3248-3265, 2012.
[32] F. Ugranli and E. Karatepe, "Multiple-distributed generation planning under load uncertainty and different penetration levels," *Electrical power and energy systems,* vol. 32, pp. 849-856, 2010.
[33] IRENA, “Renewable Power Generation Costs in 2017”, (International Renewable Energy Agency, 2018), pp. 1-160.
[34] "U.S. Solar Photovoltaic system cost benchmark", "http://www.nrel.gov", accessed Febreuary 2019.
[35] "Global inflation rate from 2012 to 2022", "https://www.statistia.com", accessed Febreuary 2019.
[36] V. P. Gountis and A. G. Bakirtis, "Efficient determination of cournot equilibria in electricity markets," IEEE transaction on power system, vol. 19, pp. 1837-1844, 2004.
[37] P. M. Subcommittee, "IEEE Reliability Test System," IEEE Transactions on Power Apparatus and Systems, Vols. PAS-98, no. 6, pp. 2047-2054, 1979.
[38] R. Nelsen, ‘An introduction to Copulas’ (Springer Press, New York, 2005, 2nd edn. 2006.
[39] D. Pfeifer and J. Neslehova, "Modeling dependence in finance and insurance: the copula approach," Blatter der DGVFM, vol. 26, pp. 177-191, 2003.